Modelling Approaches of Power Systems Considering Grid-Connected Converters and Renewable Generation Dynamics

Jaume Girona-Badia
Vinícius Albernaz Lacerda
Eduardo Prieto-Araujo
Oriol Gomis-Bellmunt
Centre d'Innovacio Tecnològica en Convertidors Estatics i Accionaments (CITCEA-UPC)
Barcelona, Spain

Stephan Kusche
Florian Pöschke
Horst Schulte
Department of Engineering I, Control Engineering
HTW Berlin - University of Applied Sciences
Berlin, Germany

***Abstract*—This paper presents a comparative analysis of several modelling approaches of key elements used in simulations of power systems with renewable energy sources. Different models of synchronous generators, transmission lines, converters, wind generators and PV power plants are compared to assess the most suitable models for grid-connection studies. It also analyses how the dynamics of PV power plants and the mechanical dynamics of wind generators affect the electrical variables on the grid side. The models were compared in terms of precision, computational time and ease of use through simulations of load connection, short-circuits, disconnection of generators and lines in a benchmark system modelled in Simulink.**

***Index Terms*—EMT simulation, mechanical dynamics, phasor simulation, power systems modelling, renewable generation dynamics.**

I. Introduction

The electrical power system is experiencing a deep penetration of renewable energy sources (RES) worldwide. Several countries have defined targets to increase the integration of RES, such as wind, solar, geothermal, hydro, ocean and biomass [1], [2], using different solutions such as DC grids, microgrids and Virtual Power Plants [3].

In order to assess how present and future power systems will perform with high penetration of RES, researchers and industry need to use proper power systems models considering a variety of technologies. However, various modelling approaches have been proposed depending on the type of study, and there is not a single choice on how to model transmission lines, synchronous generators (SGs), converters and RES.

While important recommendations and guidelines were recently available [4], [5], those are often high-level and based on the researchers' experience, and important questions still need to be addressed, such as the influence of PV power plants dynamics and mechanical dynamics of wind generators (WGs) on electrical variables and how these dynamics interact with other elements in the system.

Therefore, this paper presents a comparative analysis among several modelling approaches, considering different levels of detail of the main components of power systems with RES. It also considers the dynamics of PV power plants and mechanical dynamics of wind generators (WGs) and analyses how these dynamics affect the electrical variables on the grid side.

The remainder of this paper is organized as follows. Section II briefly introduces the models of SGs, transmission lines, converters and RES used in this study. Section III presents the methodology of the comparative analysis, including the simulated system and the tests performed. The result are shown in Section IV followed by discussions. Finally, the conclusions are drawn in Section V.

II. Modelling approaches

Synchronous generators, transmission lines, loads and converters are conventional elements used when simulating power systems with RES. Several models of converters were proposed, varying from detailed models, in the semiconductors domain, to high-level phasor models [6]. Multiple choices can also be found for synchronous generators, transmission lines and wind generators. The proper choice for each element will depend on the level of detail, the phenomena being analysed and the time available for simulation. While other studies have analysed these modelling approaches deeply focusing on specific components, it is also important to assess the interaction between them. If a very detailed transmission line model is used with an approximated generator model, the overall simulation might not be detailed enough for some specific scenarios. This interaction is covered in this paper, where groups of models are analysed together.

A. Wind turbine modelling

The wind energy system in this work is modeled as a variable-speed turbine equipped with a synchronous generator

This project has received funding from the European Union's Horizon 2020 research and innovation programme under grant agreement No 883985 (POSYTYF project).

fed by a back-to-back converter that also establishes the connection to the electrical grid. The associated aeromechanical energy conversion is nonlinear and depends on the current wind speed and the turbine states such as rotor speed or pitch angle. Different control loops govern the operation of the wind energy system with the power control of the wind energy conversion system being dominant. Depending on the current operating point and thus wind speed, the power control either maximizes the power output in partial-load region, limits the power output to rated in full-load region or generates the desired power output following a setpoint signal [7]. For the multi-MW class, the resulting closed-loop dynamics have timescales in the range of seconds [8], [9], and thus may represent relevant dynamics for the interaction with other participating units in the electrical grid.

To study the effects of including these dynamics within the power system simulation, two different models are used to display wind power. The first comprises algebraic power relations that statically portray the produced power depending on the current wind speed as only input to the model. Therein, the power produced by the wind turbine P_w is calculated using the wind speed v and a power coefficient look-up table for $c_P(\frac{\omega R}{v}, \beta)$ depending on the rotor speed ω and the pitch angle β, such that the power is given by $P_w = \frac{1}{2} c_P(\frac{\omega R}{v}, \beta) \rho \pi R^2 v^3$ [10], where R denotes the rotor radius of the wind turbine. Whenever the power output setpoint is below the extractable power of the wind, the power output of the model is immediately set to the desired value. This modeling implies a perfect control and following of the turbine states. Thus, this modeling approach neglects the dynamics when transitioning between operating points that are governed by the control loops and system characteristics such as rotor inertia or pitch dynamics.

The second model is capable of displaying the interaction of the mechanical turbine states and the control loops to form a dynamical description. It relies on the Takagi-Sugeno modeling framework that uses a convex description of linear models to describe nonlinear dynamics. To derive the model, first a linearization analysis of NREL's 5 MW reference turbine [11] using FAST [12] is conducted at several operating point within the relevant operating space. Subsequently, an observer-based controller in the Takagi-Sugeno framework is designed with respect to the aforementioned power control problem using linear matrix inequalities to derive the necessary controller gains. Further, the pitch and generator torque dynamics are modeled as first-order transfer functions to account for limited pitch rates and the generator dynamics. Details about the applied modeling and control structure can be found in [7], [9]. The model (both, open- and closed-loop) is validated using FAST and provides a proper description of the aerodynamic conversion dynamics governed by the control loops. As a result, the model-based control design directly yields a closed-loop system description that can be implemented in power system simulations capable of portraying the nonlinear dynamics inherited in the wind energy conversion process.

B. *Photovoltaic power station modelling*

In general, the photovoltaic (PV) power station consists of multiple arrays of PV cells connected to the grid via an optional DCDC converter and an inverter. Though the DCDC converter is not present in all facilities, it is used in this work because it facilitates power tracking control.

The model of one PV cell is realised as explicit single diode model, i.e. a current source (photon current i_{ph}) in parallel with a diode (diode current i_d) in parallel with a resistor (R_h) to accommodate losses [13], such that t (Kirchhoff's first law)

$$i_{pv} = i_{ph} - \underbrace{i_s \left[\exp\left(\frac{q_e v_{pv}}{A_n k_B T_c} \right) - 1 \right]}_{i_d} - \frac{v_{pv}}{R_h}. \tag{1}$$

In this form, the diode I-V characteristics is described by the theory of Shockley [14], using the Boltzmann constant k_B, elementary charge q_e and using the tunable parameters ideality factor of the diode A_n, photon current i_{ph} and saturation current i_s. The tunable parameters are fitted on the I-V and P-V characteristics of the PV cell obtained under standard test conditions (STC). The cell temperature T_c is only subject to slow changes in time and therefore assumed to be constant at the STC value of 25°C. On the other hand, the irradiation S may change rapidly, and affects the photon current following (α_T being a PV cell dependent parameter):

$$\frac{i_{ph}}{i_{ph}^{STC}} = \frac{S}{S^{STC}} \left[1 + \alpha_T (T_c - T_c^{STC}) \right]. \tag{2}$$

Agglomeration of multiple PV cells in series and parallel raises the output voltage and current. In total the PV voltage at the maximum power point (MPP) is 6.28 kV, converted to 11 kV DC voltage and power production of 90 MW peak.

Power transformation is done in a first step via a boost converter [15] and in a second step via an inverter. The boost converter is controlled via the duty cycle D, which determines the conversion ratio between PV voltage v_{pv} and DC link voltage v_{dc}. Within the continuous conduction mode, $v_{pv} = (1-D) v_{dc}$ holds [16]. A higher level controller is used to track either the MPP or demand power point (DPP) using a perturb and observe (P&O) method, e.g. [17], [18], [19]. The basic idea of this method is to perturb the PV voltage and observe the change in the power output. The direction of the voltage steps is kept if the power increases and reversed otherwise. Usually the feedback information is the PV power: $P_{pv} = v_{pv} \times i_{pv}$ (MPP). If we aim for a demanded power P_{dem}, feedback is replaced by $P_{pv}^* = -|P_{pv} - P_{dem}|$ (DPP).

C. *Synchronous machines modelling*

1) Simplified model: The simplified SG model consists of a voltage-behind-impedance model with variable frequency, governed by the swing equation. The model diagram is depicted in Fig. 1, where mechanical speed ω_m and the internal voltage E_s are calculated by

$$2H \frac{\mathrm{d}\omega_m}{\mathrm{d}t} = P_m - P_e \tag{3}$$

$$E_s = \frac{1}{1+\tau_f s} V_f \tag{4}$$

where H is the SG inertia constant, P_m is the mechanical power, P_e is the electrical power, τ_f is the field circuit time constant in p.u., and V_f is the field voltage in p.u.

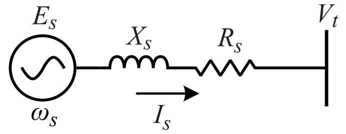

Fig. 1. Simplified SG model single-line diagram.

The first-order transfer function with time constant τ_f links the SG internal voltage to the field voltage. Adding τ_f to the simplified model allows using the same excitation system used in detailed SG models. τ_f can be calculated from the SG's field resistance and inductance or numerically by fitting a step response in the field circuit of the complete model.

2) IEEE Model 2.2: The IEEE Model 2.2 [20] is a precise yet simple electrical model in the dq axis. This model takes into account the dynamics of the stator, field, and damper windings. One of the benefits is that standard data supplied by manufacturers is usually based on the inherited parameters [20]. The equivalent circuit is represented in the rotor reference frame, depicted in Fig. 2, where the voltages are calculated as

$$v_d = \frac{\mathrm{d}\psi_d}{\mathrm{d}t} - i_d R_s - \omega_s \psi_q \tag{5a}$$
$$v_q = \frac{\mathrm{d}\psi_q}{\mathrm{d}t} - i_q R_s - \omega_s \psi_d \tag{5b}$$

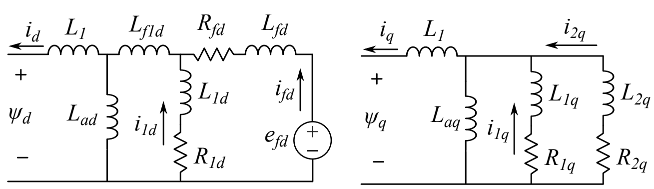

Fig. 2. IEEE Model 2.2 single-line diagram.

3) IEEE 2.2 Model with saturation: According to [20], the SG saturation significantly affects both rotor angle and excitation currents and thus should be considered in transient stability studies. In this study, the saturation was modelled as factor k added to the excitation, following the description and parameters of [21], [22].

D. Transmission lines modelling

Transmission lines play an important role in power system simulation, either by influencing steady-state power flow or by adding additional dynamics to the system. Three models were implemented in this study, described next.

1) PI model: The PI model is widely used in several power system studies due to its simplicity and suitability to model power flows and electromechanical transients. However, the PI model is only precise for a limited frequency range [23].

2) Bergeron model: The Bergeron model is also calculated for a single frequency, but it is more accurate than PI model as it uses distributed parameters and considers the travelling waves trough the lines. In this model there is no direct connection between the two line terminals. Voltages and currents at one end affect indirectly the other end after a time delay due to the travelling time.

3) Frequency-dependent model: The frequency-dependent model precisely represents the transmission line or cable throughout the whole frequency range of interest. The line resistances, inductances, capacitances and conductances are calculated from the physical line geometry and are frequency dependent. The travelling waves are accurately represented in this model and the travelling wave speed is also frequency-dependent, making it suitable to model electromagnetic transients [23].

E. Converter modelling

Several models have been proposed for the conventional two-level VSC, varying from very detailed models to high-level RMS models [6], [24]. Two models were compared in this study, described next.

1) EMT average model: One widely-used EMT model of VSCs is the average (AVG) model. The AVG model neglects the converter's high-frequency switching and considers that the VSC electrical model on the AC side is simply a controlled voltage source, defined as an amplification of the modulation index [25].

2) Phasor model: Phasor models aim to capture only the slow dynamics of the power grids, such as the electromechanical transients, with time constants generally bigger than 100 ms. In this model, the grid differential equations are substituted by algebraic equations. As the phasors are assumed to be rotating at nominal angular speed, voltages and currents have their dynamics around 0 Hz instead of 50 or 60 Hz. This allows to dramatically increase the simulation time step and consequentially the simulation speed.

In phasor simulation, the VSCs are represented as current sources with magnitude and angle defined by the control system.As phasor simulation aims mainly to speed up and simplify simulations, several approximations can be performed in the VSC control system to allow bigger simulation time steps. In this study, the reference output current given by the outer loop is directly sent to the current source, thus the output current-loop dynamics are neglected.

III. Methodology

To assess the influence of the aforementioned models, several studies were performed using an adapted Cigre European HV transmission network benchmark system [26], modelled in Simulink. The system is composed of four synchronous generators, eight transmission lines and one VSC, and represents a generic equivalent transmission system.

Table I summarizes the models simulated in each test.

1) Setpoint tracking: In this test, active and reactive power setpoints of the RES were set to 100 MW and 30 Mvar at $t = 1$ s and $t = 1$ s, respectively.

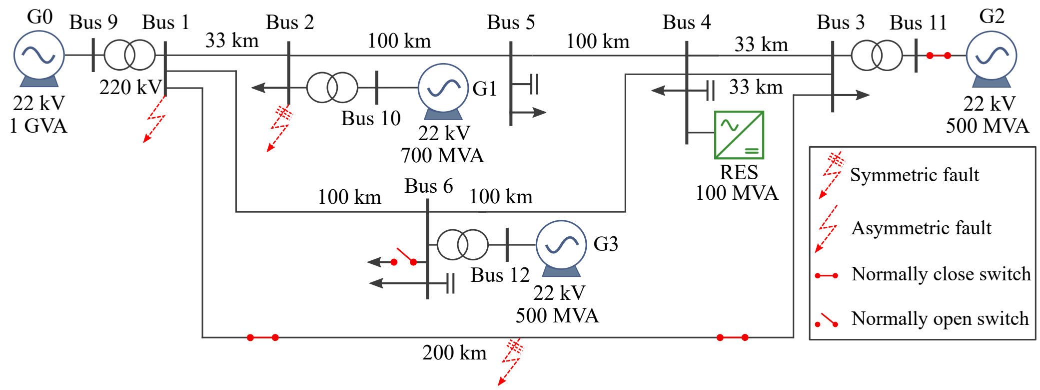

Fig. 3. Simulated system single-line diagram. Modified from [26].

2) Load connection: In this test, a 100 MW, 20 Mvar load was connected to the bus 6 at $t = 5\,s$, dropping the system frequency and voltage.

3) Symmetrical faults: In this test, a 5 Ω three-phase fault was applied to bus 2 at $t{=}5\,s$, lasting for 200 ms.

4) Asymmetrical faults: In this test, a 10 Ω mono-phase fault at phase B was applied to bus 1 at $t = 5\,s$, lasting for 500 ms.

5) Loss of generation: In this test, the generator G2 is disconnected from the system at $t = 5\,s$, producing a slow but large transient in the system.

6) Line outage: In this test, a permanent 1 Ω three-phase fault was applied to the line connecting bus 1 to bus 3. The line was isolated by two ideal circuit breakers 100 ms after the fault.

All tests were simulated using a fixed time step and the Euler method (*ode1* in Simulink). The single-line diagram of the simulated system is depicted in Fig. 3.

TABLE I
SIMULATED MODELS

Component	Model
Synchronous generator	Model 2.2 [20] with saturation **model 2.2 [20] without saturation** inertia-only model
Transmission line	Frequency-dependent (FD) model Bergeron model calculated at 50 Hz, **nominal PI model calculated at 50 Hz**
Converter	**EMT average model**, Phasor model
Renewable generation	Dynamic PV power plant, dynamic wind turbine, algebraic power laws, **ideal DC voltage source**

The tests were performed as follows. First, one model of each element (SG, transmission lines, converter, RES) was chosen to form a base group, which are indicated in bold in Table I. Afterwards, each test was performed varying one element per time in relation to the base group. This allowed to identify the influence of each model in the overall system behaviour.

Three key aspects were analysed for each model: Precision, execution time and simplicity. Finally, the key aspects were combined to express the suitability of each model for the evaluated scenarios.

IV. Results and Discussion

This section presents the simulation results, followed by discussions. Due to the extensive number of tests, only a few cases and variables are presented, which are representative of each test.

A. Influence of synchronous generator model

Figures 4-9 present active power and speed for tests 1 and 6, respectively. From Figs. 4-9 it can be observed that SGs' model 2.2 with and without saturation show a similar response. However, the system was simulated with light load, which can present optimistic results. When heavy load is simulated with contingencies, saturation should be considered. The inertia-only model, although requiring less parameters to simulate, presented more severe voltage oscillations due to the lack of damper windings. This effect is more noticeable during and post fault, as shown in Fig. 7.

The SGs' electric model slightly influenced the system's total simulation time. Model 2.2 without saturation was 12 % faster than the inertia-only model and 18.4% faster than the model 2.2 with saturation.

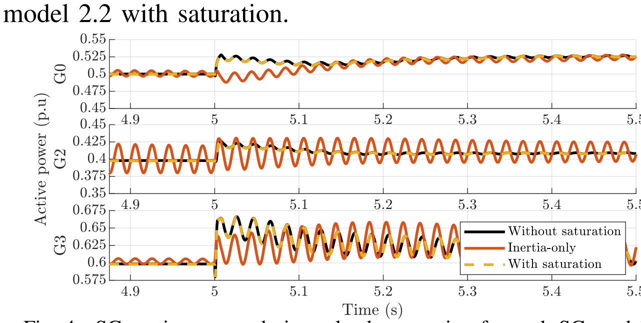

Fig. 4. SGs active power during a load connection for each SG model.

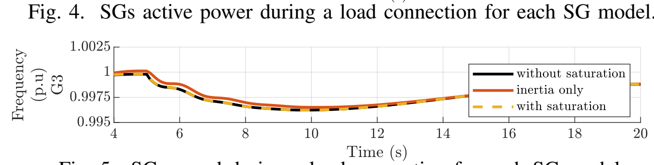

Fig. 5. SGs speed during a load connection for each SG model.

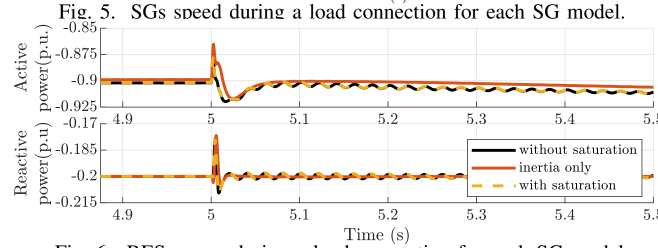

Fig. 6. RES power during a load connection for each SG model.

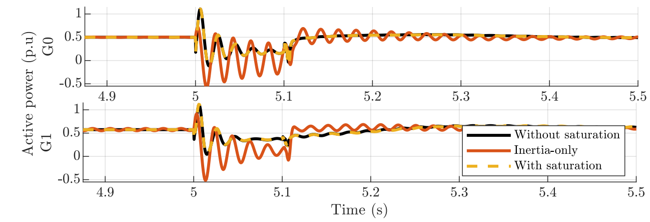

Fig. 7. SGs active power during a line outage for each SG model.

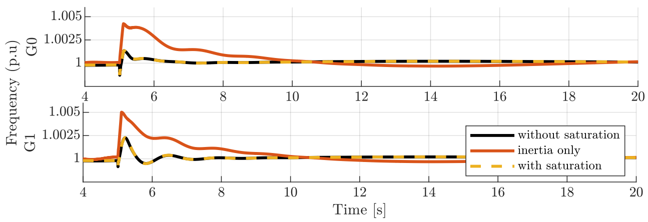

Fig. 8. SGs speed during a line outage for each SG model.

B. Influence of the transmission lines model

Figures 10-12 and 13-15 show the results for tests 2 and 3 (load connection and symmetric fault), respectively.

In can be observed in both tests that the FD model represents higher frequencies due to wave propagation and resonance frequencies. These high-frequency components are also present though less represented in the Bergeron model and almost absent in PI nominal. However, the same low-frequency tendency is well represented in the three models. The fastest simulation was performed with the PI model, followed by the Bergeron model 16% slower on average than the the simulation with PI model. The FD model resulted in simulations 2113.6% slower than the PI model on average.

Therefore, the PI model would be adequate if essentially electromechanical transients are simulated. Using high-order models would add minor precision at the cost of a larger simulation time. Nevertheless, if electromagnetic transients are simulated or if the converter switching or control dynamics are a concern, the PI model might under-represent important high-frequency components, yielding optimistic results. The Bergeron model might be adequate between both extremes, where the nominal frequency dominates the response but the simulated lines' length are too large to neglect travelling wave effects. These guidelines might change for underground cables as their frequency-dependent behaviour is more significant.

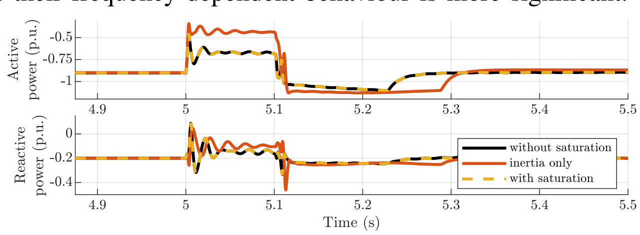

Fig. 9. RES power during a line outage for each SG model.

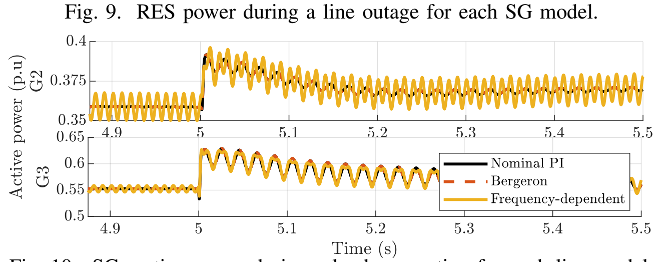

Fig. 10. SGs active power during a load connection for each line model.

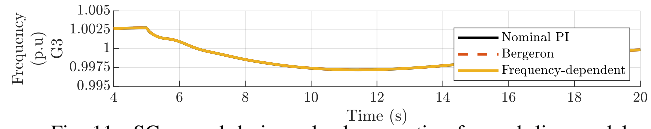

Fig. 11. SGs speed during a load connection for each line model.

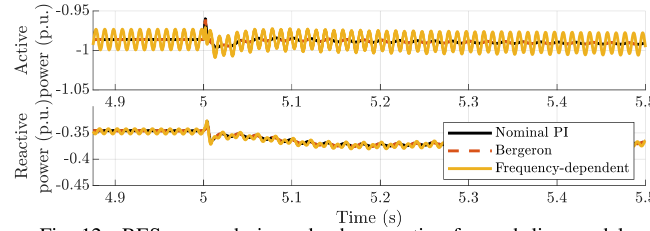

Fig. 12. RES power during a load connection for each line model.

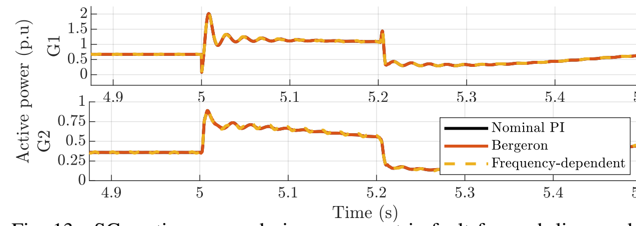

Fig. 13. SGs active power during a symmetric fault for each line model.

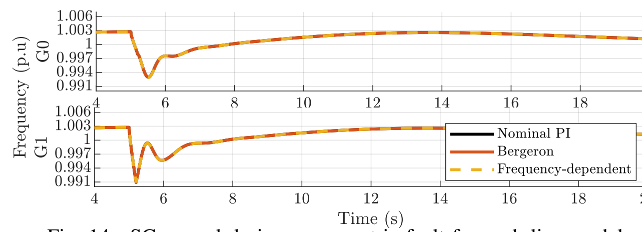

Fig. 14. SGs speed during a symmetric fault for each line model.

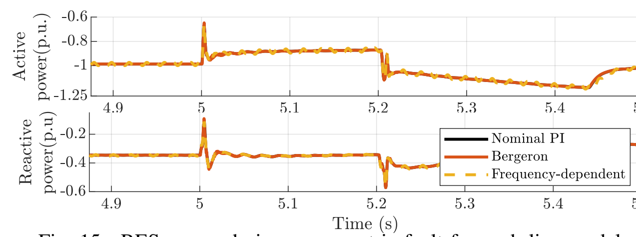

Fig. 15. RES power during a symmetric fault for each line model.

C. Influence of the converter model

Figures 16-22 show the results for tests 1, 4 and 5 (setpoint tracking, asymmetric fault and loss of generation), respectively.

In the setpoint tracking test, the VSC output power was nearly the same in both EMT and Phasor models.

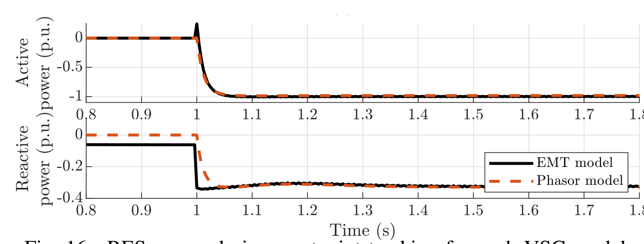

Fig. 16. RES power during a setpoint tracking for each VSC model.

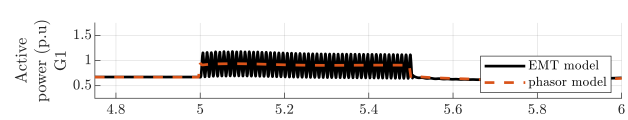

Fig. 17. SG active power during an asymmetric fault for each VSC model.

During the asymmetric fault, SGs in EMT model showed an oscillatory torque produced by the transient, where only the average value is captured by the phasor model (Fig. 17). However, it should be highlighted that this effect is due to the simulation type (EMT or Phasor), and not due to the VSC model. Similar behaviour can be observed in the RES output power (Fig. 19).

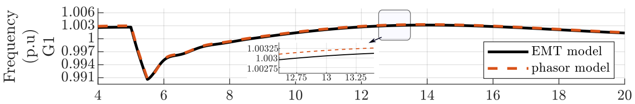

Fig. 18. SG speed during an asymmetric fault for each VSC model.

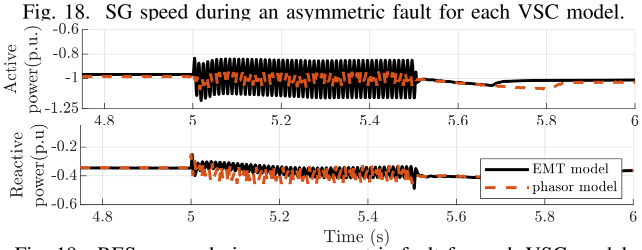

Fig. 19. RES power during an asymmetric fault for each VSC model.

In the generator disconnection test, both EMT and phasor models presented similar responses, despite for an offset in the SGs speed (Fig. 20-22). This slight deviation in the phasor model might be due to model approximations as the stator fluxes derivatives are neglected.

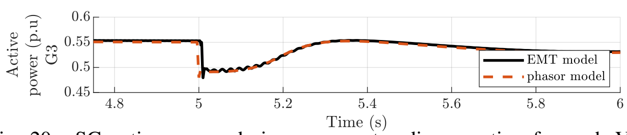

Fig. 20. SG active power during a generator disconnection for each VSC model.

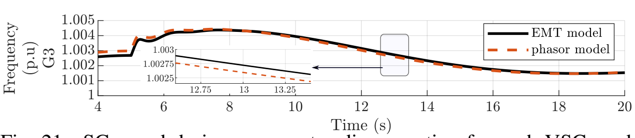

Fig. 21. SG speed during a generator disconnection for each VSC model.

The proper choice on using EMT or Phasor models will depend on the type of study and the system's size. Studies on small systems, focused on fast dynamics such as modulation and control studies, dynamic analysis of the PLL or detailed short circuit studies might require EMT simulation. On the other hand, studies on large systems, where electromechanical variables are being analysed, can be precisely simulated using phasor models in a fraction of the EMT simulation time. In the tests performed, the simulation with phasor models was 1277% faster in average when compared to simulations with EMT models.

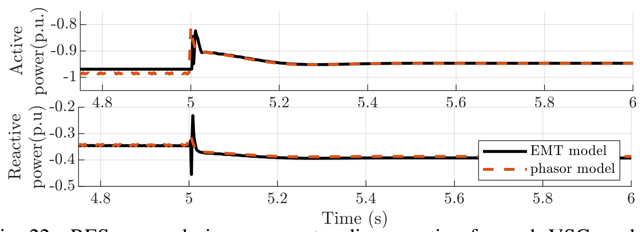

Fig. 22. RES power during a generator disconnection for each VSC model.

D. Influence of RES

Figures 23-28 show the results for tests 3 and 4 (symmetric and asymmetric faults), respectively. By analysing the results, it can be observed that the RES model had minor influence on the SGs variables during short-circuit tests. This was observed because the RES dynamics are slower and consequently do not produce significant deviations during the short period of the fault.

In the VSC output power, a noticeable difference between the RES models could be observed.

But in the VSC power, the difference is noticeable, especially post-fault.

The fastest simulation was performed using the ideal DC source model, followed by static PV, which was 72,5% slower, followed by the static wind, which was 85,39 % slower than the ideal DC source. Finally, the slowest models were the dynamic PV (106.1% slower than the ideal DC source) and the dynamic wind (164.82% slower than the ideal DC source).

Therefore for studies in systems with low-share of RES and dominated by SGs, the ideal DC source would provide adequate accuracy. Conversely, for studies in systems with high-share of RES, static and dynamic models should be used. Static models are good options as they are faster to simulate than dynamic models and provide a similar response to those in several events.

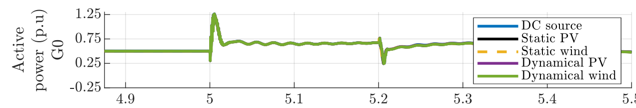

Fig. 23. SG active power during a symmetric fault for each RES model.

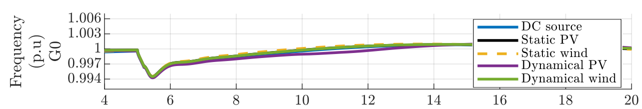

Fig. 24. SG speed during a symmetric fault each RES model.

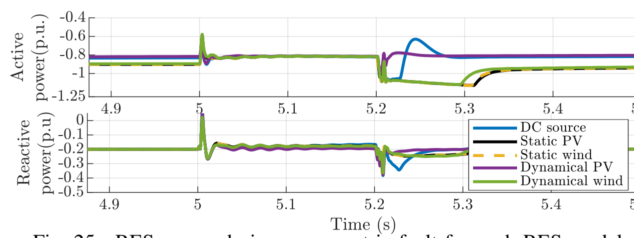

Fig. 25. RES power during a symmetric fault for each RES model.

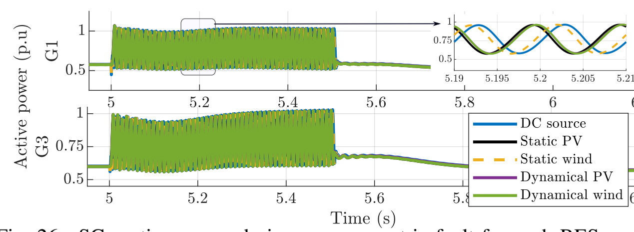

Fig. 26. SGs active power during an asymmetric fault for each RES model.

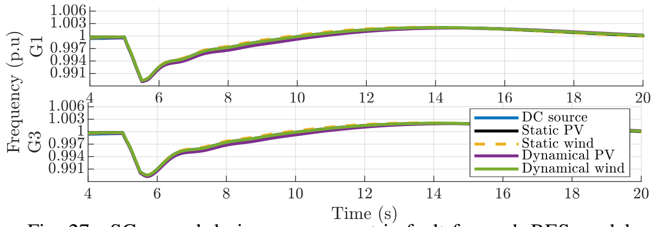

Fig. 27. SGs speed during an asymmetric fault for each RES model.

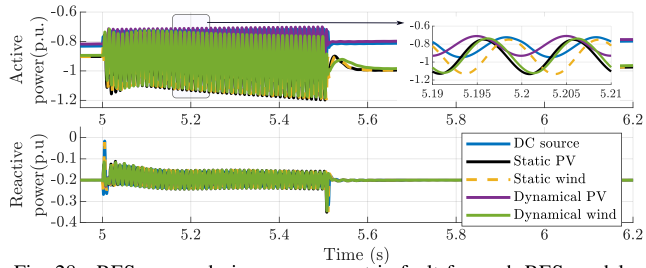

Fig. 28. RES power during an asymmetric fault for each RES model.

V. Conclusion

This paper presented a comparative analysis amongst several models currently used to simulate power systems with RES in transient stability studies. Several models of SGs, transmission lines, converters and RES were compared in terms of precision and computational time. The simulated benchmark system was generic and could well represent typical transmission systems.

From the tests performed, it could be observed that the most suitable models for the study of an electromechanical events in the system tested were: the Model 2.2 [20] without saturation, nominal PI model, phasor model and ideal DC voltage source. These models were able to track the fundamental components of the variables been simulated and at the same time have less computational burden. However, if the system or the study purpose changes, the best models will change. For example, a system with high load might require modelling SG saturation to achieve a precise response. Moreover, If the converter switching is modelled, a frequency-dependent transmission line model would be needed to represent precisely the high-frequency components associated with the switching. The EMT model represents fast oscillations needed for fast dynamic studies. In this study, the SGs dominate the system presented. However, if the share of RES increases, the RES model dynamics will have a more significant influence on the electromechanical events and thus dynamic RES models should be used.

References

[1] European Comission, “Energy roadmap 2050,” Luxembourg: Publications Office of the European Union, Tech. Rep., 2012.

[2] European Council, “Directive 2009/28/EC of the European Parliament and of the Council of 23 April 2009 on the promotion of the use of energy from renewable sources,” Brussels, Belgium, Tech. Rep., 2009.

[3] B. Marinescu, O. Gomis-Bellmunt, F. Dörfler, H. Schulte, and L. Sigrist, “Dynamic virtual power plant: A new concept for grid integration of renewable energy sources,” *arXiv:2108.00153*, 2021.

[4] G. D. Carne, M. Liserre, M. Langwasser, M. Ndreko, R. Bachmann, R. W. D. Doncker, R. Dimitrovski, B. J. Mortimer, A. Neufeld, and F. Rojas, “Which deepness class is suited for modeling power electronics?: A guide for choosing the right model for grid-integration studies,” *IEEE Industrial Electronics Magazine*, vol. 13, no. 2, pp. 41–55, jun 2019.

[5] M. Paolone, T. Gaunt, X. Guillaud, M. Liserre, S. Meliopoulos, A. Monti, T. V. Cutsem, V. Vittal, and C. Vournas, “Fundamentals of power systems modelling in the presence of converter-interfaced generation,” *Electric Power Systems Research*, vol. 189, p. 106811, dec 2020.

[6] CIGRE Working Group B4-57, *Technical Brochure 604: Guide for the Development of Models for HVDC Converters in a HVDC Grid*. CIGRE, 2014.

[7] F. Pöschke, E. Gauterin, M. Kühn, J. Fortmann, and H. Schulte, “Load mitigation and power tracking capability for wind turbines using linear matrix inequality-based control design,” *Wind Energy*, 2020, dOI: 10.1002/we.2516.

[8] J. Bjork, D. V. Pombo, and K. H. Johansson, “Variable-speed wind turbine control designed for coordinated fast frequency reserves,” *IEEE Transactions on Power Systems*, p. 1–1, 2021. [Online]. Available: http://dx.doi.org/10.1109/TPWRS.2021.3104905

[9] F. Pöschke and H. Schulte, “Evaluation of different apc operating strategies considering turbine loading and power dynamics for grid support,” *Wind Energy Science Discussions*, vol. 2021, pp. 1–14, 2021. [Online]. Available: https://wes.copernicus.org/preprints/wes-2021-80/

[10] M. Hansen, *Aerodynamics of Wind Turbines*. Routledge, 2015.

[11] J. M. Jonkman, S. Butterfield, W. Musial, and G. Scott, “Definition of a 5-MW Reference Wind Turbine for Offshore System Development,” National Renewable Energy Laboratory, Tech. Rep., 2009.

[12] J. M. Jonkman and M. L. Buhl, “FAST Users Guide,” National Renewable Energy Laboratory, Tech. Rep., 2005.

[13] W. Xiao, *Photovoltaic Power System: Modeling, Design, and Control*. Wiley, 2017.

[14] W. Shockley, “The theory of p-n junctions in semiconductors and p-n junction transistors,” *The Bell System Technical Journal*, vol. 28, no. 3, pp. 435–489, 1949.

[15] R. W. Erickson, “DC–DC Power Converters,” in *Wiley Encyclopedia of Electrical and Electronics Engineering*. American Cancer Society, 2007.

[16] R. W. Erickson and D. Maksimovic, *Fundamentals of Power Electronics*, 2nd ed. Springer US, 2001.

[17] W. Teulings, J. Marpinard, A. Capel, and D. O’Sullivan, “A new maximum power point tracking system,” in *Proceedings of IEEE Power Electronics Specialist Conference - PESC ’93*, Jun. 1993, pp. 833–838.

[18] Y. Kim, H. Jo, and D. Kim, “A new peak power tracker for cost-effective photovoltaic power system,” in *IECEC 96. Proceedings of the 31st Intersociety Energy Conversion Engineering Conference*, vol. 3, Aug. 1996, pp. 1673–1678 vol.3, iSSN: 1089-3547.

[19] N. Femia, G. Petrone, G. Spagnuolo, and M. Vitelli, “Optimization of perturb and observe maximum power point tracking method,” *IEEE Transactions on Power Electronics*, vol. 20, no. 4, pp. 963–973, Jul. 2005.

[20] IEEE, *Std 1110-2019 - IEEE Guide for Synchronous Generator Modeling Practices and Parameter Verification with Applications in Power System Stability Analyses*.

[21] T. V. Cutsem and L. Papangelis, “Description, Modeling and Simulation Results of a Test System for Voltage Stability Analysis,” University of Liège, Belgium, Tech. Rep., 2013.

[22] T. Van Cutsem, M. Glavic, W. Rosehart, C. Canizares, M. Kanatas, L. Lima, F. Milano, L. Papangelis, R. A. Ramos, J. A. d. Santos, B. Tamimi, G. Taranto, and C. Vournas, “Test systems for voltage stability studies,” *IEEE Transactions on Power Systems*, vol. 35, no. 5, pp. 4078–4087, 2020.

[23] N. Watson and J. Arrillaga, *Power Systems Electromagnetic Transients Simulation, 2nd ed.* Institution of Engineering and Technology, 2018.

[24] S. Khan and E. Tedeschi, “Modeling of MMC for fast and accurate simulation of electromagnetic transients: A review,” *Energies*, vol. 10, no. 8, p. 1161, aug 2017.

[25] W. Lu and B.-T. Ooi, “Optimal acquisition and aggregation of offshore wind power by multiterminal voltage-source HVDC,” *IEEE Transactions on Power Delivery*, vol. 18, no. 1, pp. 201–206, jan 2003.

[26] CIGRE Task Force C6-04, *Technical Brochure 575: Benchmark Systems for Network Integration of Renewable and Distributed Energy Resources*. CIGRE, 2014.